Development and characterization of anti-biofilm coatings applied by Non-Equilibrium Atmospheric Plasma on stainless steel

Paula Fernández-Gómez*[(a)], Ignacio Muro-Fraguas*[(b)], Rodolfo Múgica-Vidal**[(b)], Ana Sainz-García[(b)], Elisa Sainz-García[(b)], Montserrat González-Raurich[(a)], Avelino Álvarez-Ordóñez[(a)], Miguel Prieto[(a)], Mercedes López[(a)], María López[(c)], Paula Toledano[(c)], Yolanda Sáenz[(c)], Ana González-Marcos[(b)], Fernando Alba-Elías[(b)]

[(a)] Department of Food Hygiene and Technology and Institute of Food Science and Technology, Universidad de León, León, Spain
[(b)] Department of Mechanical Engineering, University of La Rioja, Logroño, Spain
[(c)] Molecular Microbiology Area, Center for Biomedical Research of La Rioja (CIBIR), Logroño, Spain

* These authors contributed equally to this work
** Corresponding author

Declarations of interest: none

Accepted Version for publication in Food Research International
Link to publisher version (DOI): https://doi.org/10.1016/J.FOODRES.2020.109891

Published source citation:
Fernández-Gómez, P., Muro-Fraguas, I., Múgica-Vidal, R., Sainz-García, A., Sainz-García, E., González-Raurich, M., Álvarez-Ordóñez, A., Prieto, M., López, M., López, M., Toledano, P., Sáenz, Y., González-Marcos, A., & Alba-Elías, F. (2022). Development and characterization of anti-biofilm coatings applied by Non-Equilibrium Atmospheric Plasma on stainless steel. *Food Research International*, *152*. https://doi.org/10.1016/J.FOODRES.2020.109891

Author names and affiliations:

Paula Fernández-Gómez*
Department of Food Hygiene and Technology and Institute of Food Science and Technology
Universidad de León
Campus de Vegazana s/n, 24071 - León, Castilla y León, Spain
Tel.: +34 987293452
E-mail address: pafeg@unileon.es

Ignacio Muro-Fraguas*
Department of Mechanical Engineering
University of La Rioja
C/ San José de Calasanz 31, 26004 - Logroño, La Rioja, Spain
Tel.: +34 941299276
E-mail address: ignacio.muro@unirioja.es

Ana Sainz-García
Department of Mechanical Engineering
University of La Rioja
C/ San José de Calasanz 31, 26004 - Logroño, La Rioja, Spain
Tel.: +34 941299276

E-mail address: ana.sainz@unirioja.es

Elisa Sainz-García
Department of Mechanical Engineering
University of La Rioja
C/ San José de Calasanz 31, 26004 - Logroño, La Rioja, Spain
Tel.: +34 941299276
E-mail address: elisa.sainzg@unirioja.es

Montserrat González-Raurich
Department of Food Hygiene and Technology and Institute of Food Science and Technology
Universidad de León
Campus de Vegazana s/n, 24071 - León, Castilla y León, Spain
Tel.: +34 987293452
E-mail address: mmgonr@unileon.es

Avelino Álvarez-Ordóñez
Department of Food Hygiene and Technology and Institute of Food Science and Technology
Universidad de León
Campus de Vegazana s/n, 24071 - León, Castilla y León, Spain
Tel.: +34 987293452
E-mail address: aalvo@unileon.es

Miguel Prieto
Department of Food Hygiene and Technology and Institute of Food Science and Technology
Universidad de León
Campus de Vegazana s/n, 24071 - León, Castilla y León, Spain
Tel.: +34 987293452
E-mail address: miguel.prieto@unileon.es

Mercedes López
Department of Food Hygiene and Technology and Institute of Food Science and Technology
Universidad de León
Campus de Vegazana s/n, 24071 - León, Castilla y León, Spain
Tel.: +34 987293452
E-mail address: mmlopf@unileon.es

María López
Molecular Microbiology Area
Center for Biomedical Research of La Rioja (CIBIR)
C/ Piqueras 98, 26006 - Logroño, La Rioja, Spain
Tel.: +34 941278791
E-mail address: mlopezm@riojasalud.es

Paula Toledano
Molecular Microbiology Area
Center for Biomedical Research of La Rioja (CIBIR)
C/ Piqueras 98, 26006 - Logroño, La Rioja, Spain
Tel.: +34 941278791
E-mail address: ptoledano@riojasalud.es

Yolanda Sáenz
Molecular Microbiology Area
Center for Biomedical Research of La Rioja (CIBIR)
C/ Piqueras 98, 26006 - Logroño, La Rioja, Spain
Tel.: +34 941278791
E-mail address: ysaenz@riojasalud.es

Ana González-Marcos

Department of Mechanical Engineering
University of La Rioja
C/ San José de Calasanz 31, 26004 - Logroño, La Rioja, Spain
Tel.: +34 941299519
E-mail address: ana.gonzalez@unirioja.es

Fernando Alba-Elías
Department of Mechanical Engineering
University of La Rioja
C/ San José de Calasanz 31, 26004 - Logroño, La Rioja, Spain
Tel.: +34 941299276
E-mail address: fernando.alba@unirioja.es

Corresponding author:

Rodolfo Múgica-Vidal**
Department of Mechanical Engineering
University of La Rioja
C/ San José de Calasanz 31, 26004 - Logroño, La Rioja, Spain
Tel.: +34 941299276
E-mail address: rodolfo.mugica@unirioja.es

ABSTRACT

Biofilm-mediated microbial persistence of pathogenic and spoilage bacteria is a serious problem in food industries. Due to the difficulty of removing mature biofilms, great efforts are being made to find new strategies to prevent bacterial adherence to surfaces, the first step for biofilm development. In this study, coatings of (3-aminopropyl)triethoxysilane (APTES), tetraethyl orthosilicate (TEOS) and acrylic acid (AA) were applied by Non-Equilibrium Atmospheric Plasma on stainless steel (SS) AISI 316, the SS most commonly used in food industry equipment. Their anti-biofilm activity was assessed against *Listeria monocytogenes* CECT911 and *Escherichia coli* CECT515 after incubation at 37 °C. The best results were obtained for *L. monocytogenes*, with coatings consisting of a base coating of APTES and a functional coating of TEOS (AP10+TE6) or AA (AP10+AA6) that reduced biofilm production by 45% and 74%, respectively, when compared with the uncoated SS. These coatings were further characterized, together with a variation of the best one that replaced the acrylic acid with succinic acid (AP10+SA6). Their anti-biofilm activity was assessed under different incubation conditions, including two strains of *L. monocytogenes* isolated from processing environments of a meat industry. The coating AP10+AA6 reduced the biofilm formation by 90% after incubation at 12 °C, a temperature more representative of those commonly found in food processing environments. The morphological and physico-chemical characterization of the selected coatings showed that the coating with the highest anti-biofilm activity (i.e., AP10+AA6) had lower surface roughness and higher hydrophilicity. This suggests that the formation of a hydration layer prevents the adherence of *L. monocytogenes*, an effect that seems to be enhanced by low temperature conditions, when the wettability of the strains is increased.

Keywords: Surface modification; Stainless steel; Atmospheric pressure cold plasma; Plasma-polymerization; Anti-biofilm coatings; Hydration layer; *Listeria monocytogenes*

1. INTRODUCTION

The persistence of pathogenic and spoilage microorganisms in the production environment is a serious concern for food business operators and Public Health authorities. The ability of microorganisms to survive for long periods of time in certain food processing environments has been related to various factors, including their survival at refrigeration temperatures and desiccation conditions, resistance to disinfectants, or the development of biofilms (Rodríguez-López, Rodríguez-Herrera, Vázquez-Sánchez, & López Cabo, 2018). The microbial colonization of tools, surfaces and equipment in the form of biofilms may lead to the cross contamination of food products, which can ultimately result in important economic losses for producers and increased health risks for consumers (Alvarez-Ordóñez, Coughlan, Briandet, & Cotter, 2019; Larsen et al., 2014).

Conventional methods used for cleaning and disinfection in food industries are often ineffective towards mature biofilms as bacteria encased in biofilms are more resistant to different stress conditions and antimicrobial agents than bacteria in planktonic state (Günther, Scherrer, Kaiser, Derosa, & Mutters, 2016; Pan, Breidt, & Kathariou, 2006). Due to its ease of application, disinfectants like hypochlorites, iodophors, oxidizing agents, alcohols, quaternary ammonium and acid compounds are among the most commonly used biofilm control agents. However, they do not achieve a complete elimination of bacterial biofilms and they rely in a previous disruption of the biofilm polymeric matrix through the use of efficient cleaning agents in order to reach the bacteria. In addition, an inadequate use of disinfectants might imply risks for human health and the environment, with the possible generation of bacterial resistance or tolerance phenomena (Langsrud, Sidhu, Heir, & Holck, 2003; Skowron et al., 2019).

Since biofilms are difficult to remove, great efforts are being made to find new strategies to prevent biofilm development. These approaches focus either on reducing bacterial adherence to surfaces, which is the first step in biofilm formation, or on killing the bacteria once they are attached to the surface. In order to achieve an anti-biofilm effect, equipment and food contact surfaces can be modified with coatings that contain and release biocidal agents, immobilize an antibacterial agent or change the physico-chemical properties of the surface. This latter strategy is based upon the synergistic effect of a chemical modification (change of hydrophobicity, electronegativity, etc.) and a morphological modification (change of roughness, generation of nano- or micro-structures, etc.) of the surface to reduce microbial attachment (Cao et al., 2018; Coughlan, Cotter, Hill, & Alvarez-Ordóñez, 2016; Faure et al., 2012; Friedlander, Nir, Reches, & Shemesh, 2019; Zhong, Pang, Che, Wu, & Chen, 2013). Unlike antimicrobial coatings, the physico-chemical modification of surfaces is a less expensive approach, can produce a more durable anti-biofilm effect and does not generate microbial resistance. This makes its implementation in the food industry more feasible (Bazaka, Jacob, Chrzanowski, & Ostrikov, 2015; Cattò, Villa, & Cappitelli, 2018).

Non-Equilibrium Atmospheric Plasma has become a promising technology for coating deposition and surface modification (Da Ponte et al., 2011, 2012; Xu et al., 2015). Among its advantages are that it is a

solvent-free process that only requires reduced amounts of chemical precursor(s), it does not need to work under vacuum, it works at mild temperatures and it is easily scalable for industrial applications. These characteristics make it a more economical and environmentally friendly technology. In addition, it allows, through the control of different processing parameters, the production of coatings with different characteristics and, therefore, anti-biofilm potential (Cattò et al., 2018; Múgica-Vidal et al., 2019; Sardella, Palumbo, Camporeale, & Favia, 2016). The application of this type of coatings on stainless steel, the material most commonly used in food industries (Dürr, 2007), has previously shown promising anti-biofilm results (Li, 2016; Ma et al., 2012).

Different types of precursors have been previously used to deposit coatings with anti-biofilm properties. Stallard, McDonnell, Onayemi, O'Gara, & Dowling (2012) used an Atmospheric Pressure Plasma Jet (APPJ) system for the plasma-polymerization of tetraethyl orthosilicate (TEOS), hexamethyldisiloxane (HMDSO), and a mixture of tetramethylcyclotetrasiloxane (TMCTS) and perfluorooctytriethoxysilane (PFOTES) on silicon wafers. They observed that superhydrophilic and superhydrophobic coatings showed a reduced protein adhesion in comparison with that observed for hydrophobic surfaces. Furthermore, a superhydrophobic coating deposited on titanium coupons reduced the adhesion of *Staphylococcus aureus*. Villanueva, Salinas, Copello, & Díaz (2014) coated aluminium alloy plates with TEOS and 3-mercaptopropyltrimethoxysilane (MPTMS) in a sol-gel process and observed a reduction in the attachment of *Pseudomonas aeruginosa* that was attributed to an electrostatic repulsion between the coating and the bacteria. Also, several authors have reported antibacterial effects associated with the use of acrylic acid (AA) for surface modification. AA grafting on polypropylene nonwoven fabric and on poly(ethylene terephthalate) (PET) films through gamma-ray copolymerization has been reported to increase hydrophilicity and improve antibacterial activity. Also, copolymers synthesized with poly(acrylic acid) (PAA), poly(styrene) (PS) and poly(methyl methacrylate) (PMMA) have shown antimicrobial effects against *S. aureus*, *Escherichia coli* and *P. aeruginosa*. These bactericidal and bacterial adhesion inhibitory effects have been attributed to the carboxylic groups present in AA (Gratzl, Paulik, Hild, Guggenbichler, & Lackner, 2014; Ping, Wang, & Xuewu, 2011; Yang, Lin, Wu, & Chen, 2003)**.**

In this study, coatings of different chemical nature (APTES, AA and TEOS) and morphology were applied through Non-Equilibrium Atmospheric Plasma on stainless steel (SS) AISI 316. The anti-biofilm efficacy of the coatings was assessed against *Listeria monocytogenes* and *E. coli*, two major foodborne pathogenic microorganisms. Listeriosis is one of the most serious food-borne diseases under EU surveillance, with an increasing trend of confirmed cases in the EU/EAA observed in recent years and a case fatality of 15.6%. Also, an increase in the confirmed cases of Shiga toxin producing *E. coli* infection in humans has been reported, both from foodborne and waterborne outbreaks (EFSA & ECDC, 2019). In the first place, simpler coatings made of only one precursor (TEOS or AA) were tested. These were applied by varying the number of passes and the plasma-deposition configuration. Later on, in order to improve the anti-biofilm activity

and mechanical resistance and shelf-life of the coatings, composed coatings made of a base coating and a functional coating of different precursors were also tested. A selection of the coatings with the most promising anti-biofilm activity was further tested on three *L. monocytogenes* strains, due to the special concern this pathogenic microorganism poses to the food industry (Colagiorgi et al., 2017; Rodríguez-López et al., 2018), and under conditions that better resemble those prevailing during food processing. Furthermore, for the selected coatings, a thorough morphological and physico-chemical characterization was performed, which included Atomic Force Microscopy (AFM), Scanning Electron Microscopy (SEM), X-Ray Photoelectron Spectroscopy (XPS) and Water Contact Angle (WCA) analyses.

2. MATERIALS AND METHODS

2.1. Bacterial strains, media and culture conditions

The bacterial isolates used in this study are the reference strains from the Spanish Type Culture Collection (CECT) *E. coli* CECT515 and *L. monocytogenes* CECT911 (serotype 1/2c), and two *L. monocytogenes* strains previously isolated from the processing environment of a meat industry (ULE1264, serotype 1/2a; and ULE1265, serotype 1/2c). All strains were maintained at -20 ^{o}C in cryovials with 40% of glycerol as cryoprotectant and were recovered by streaking them on Brain Heart Infusion (BHI) agar (Merck, Germany) plates. After incubation at 37 ^{o}C for 24 hours under aerobic conditions, the plates were stored at 4 ^{o}C. For bacterial inoculum preparation, a single colony from the BHI agar plates was inoculated in tubes with 10 mL of BHI broth (Merck, Germany), which were also incubated at 37 ^{o}C for 24 hours.

2.2. Non-Equilibrium Atmospheric Plasma coating deposition

Custom Ø 35 mm SS AISI 316 plates were coated through plasma-polymerization with an APPJ system PlasmaSpot500® (MPG, Luxembourg) (**Figure 1(A)**), which consists of two coaxial, cylindrical electrodes (the external one connected to a high voltage source and the internal one grounded) with an Al_2O_3 dielectric barrier between them. As schematized in **Figure 1(B)**, the plasma jet is generated from a flow of gas (plasma gas) that is excited by the electromagnetic field between the electrodes. For the plasma-polymerization of coatings, an atomized liquid precursor is added to the plasma jet through an exit at the end of the inner electrode. In order to facilitate the deposition of the coatings, the plates were previously activated by exposing them to one pass of the APPJ without adding any precursor and with the same parameters used in the subsequent coating stage. As shown in **Table 1**, a wide variety of coatings were deposited by modifying the following processing parameters: plasma gas, carrier gas flow for the precursor, plasma power, gap between the plasma gun and the top of the plates (**Figure 1(C)**), plasma gun speed, precursor liquid and number of passes. Also, two different shapes of the exit at the end of the inner electrode were used: an umbrella shape (**Figure 1(D1)**) that releases the atomized precursor perpendicularly to the plasma jet, and a tube shape (**Figure 1(D2)**) that releases the atomized precursor parallel to the plasma jet. All coatings were applied using a scanning pattern with a pitch of 2 mm, a plasma gas flow of 80 slm and a frequency of 68 kHz. The liquid precursors tested were

3-aminopropyltriethoxysilane (APTES), acrylic acid (AA), tetraethyl orthosilicate (TEOS) and a 0.3M solution of succinic acid (SA).

2.3. Assessment of the anti-biofilm activity of the coatings

Biofilm formation assays were performed on coated and uncoated (positive control) custom Ø 35 mm SS AISI 316 plates. Bacterial suspensions containing ~10^6 CFU/mL were prepared by diluting the bacterial inoculum in fresh BHI broth. Then, 4 mL of these suspensions were inoculated into each SS plate. The experiments were always run with coated SS plates and uncoated SS plates in parallel. Four replicates were made for each strain and coating and a negative control with non-inoculated BHI broth was also included in all experiments. During the initial screening of the coatings, SS plates were incubated at 37 ^{o}C for 24 hours. From the biofilm formation results of this screening, the most promising coatings were selected for the morphological and physico-chemical characterization that is described in section 2.6, and for a second stage of biofilm formation assays. The coated and uncoated SS plates that were used for this second stage were incubated under the same conditions that had been used in the initial screening (37 ^{o}C / 24 hours) and three additional conditions: 37 ^{o}C / 48 hours, 12 ^{o}C / 144 hours and 12 ^{o}C / 288 hours. The incubation conditions at a lower temperature of 12 ^{o}C for longer times (144 and 288 hours) were added in the second stage of biofilm formation assays because these are more accurate representations of the conditions prevailing during food processing. During this second stage, three strains of *L. monocytogenes* were used (CECT911, ULE1264 and ULE1265). Following incubation, biofilm formation was assessed following the protocol described by Ma et al. (2012) with minor modifications: the plates were washed three times with Ringer buffer (Merck), the biofilm was stained for 15 minutes with 4 mL of a 0.1% crystal violet (Panreac, Spain) solution and the excess of stain was removed by washing the plates three times with Ringer buffer. Then, 5 mL of 95% ethanol were added to each plate in order to dissolve the cell bound crystal violet, and after 15 minutes the optical density (OD) at 595 nm was measured using a spectrophotometer (UV-3100PC, VWR, USA)**.** For each coating tested, the relative biofilm production (%) was calculated as follows:

Relative biofilm production = (OD_{595} coating / OD_{595} SS) * 100

Where:

OD_{595} coating = mean OD_{595} for inoculated coated plates - mean OD_{595} for non-inoculated control coated plates.

OD_{595} SS = mean OD_{595} for inoculated uncoated SS plates - mean OD_{595} for non-inoculated control uncoated SS plates.

Values of relative biofilm production lower than 100% indicate a potential anti-biofilm activity and values higher than 100% indicate a potential pro-biofilm activity of the tested coatings.

2.4. Visualization of biofilms by scanning electron microscopy (SEM)

For SEM analysis, biofilms were grown on coated and uncoated Ø 35 mm SS AISI 316 plates for 24 hours at 37 °C or for 144 hours at 12 °C, following the approach previously described. After incubation, the plates were washed twice with Ringer buffer, biofilms were fixed with 2.5% glutaraldehyde phosphate buffered saline (TAAB Laboratories, UK) for 2 hours at 4 °C and washed three times with phosphate buffered saline (PBS). The samples were then treated with 2% osmium tetroxide PBS (TAAB Laboratories, UK) for 2 hours, washed again three times with PBS and dehydrated in increasing concentrations of ethanol (Panreac): 30% (30 min), 50% (30 min), 70% (30 min), 90% (30 min), 3 x 96% (30 min) and 3 x 100% (30 min). Afterwards, the samples were dried using a CPD 030 critical point dryer (BAL-TEC Inc., Liechtenstein) and immediately coated with gold (BALZERS sputter coater SCD 004, Liechtenstein). SEM preparations were observed under a JEOL JSM-6480 LV scanning electron microscope (JEOL, Japan).

2.5. Determination of the cellular hydrophobicity

The cellular hydrophobicity for the bacterial strains was determined with an adhesion-to-hydrocarbon method following the protocol described by Hsu, Fang, Borca-Tasciuc, Worobo, & Moraru (2013) with minor modifications. Briefly, bacterial cultures grown for 24 hours at 37 °C and for 144 hours at 12 °C were harvested by centrifugation at 3100 x g for 10 min at 4 °C and resuspended in a Ringer buffer solution to obtain suspensions with a standardized microbial load (OD_{600} = 0.35 ± 0.01; ~10^8 CFU/mL). Then, 3 mL of the standardized bacterial suspensions were aliquoted in three tubes and 0.75 mL of hexadecane (VWR) were added to two of them, leaving the third one as a control. The tubes were incubated for 10 min at 37 °C, vortexed for 10 seconds and incubated for 30 min at 37 °C. The migration of the bacterial cells from the aqueous bacterial suspension to the hydrocarbon was determined by measuring the differences in optical density at 540 nm between the bacterial suspensions incubated with and without hexadecane. The hydrophobicity of the strains was expressed as a percentage, calculated as follows:

Cell hydrophobicity (%) = (1 - (OD_{450} hexadecane / OD_{450} control)) * 100

Values closer to 0% indicate a high hydrophilicity (or affinity for the aqueous phase) and values closer to 100% indicate a high hydrophobicity (or affinity for the hydrocarbon).

2.6. Morphological and physico-chemical characterization of the coatings

The morphological characterization of the coatings was conducted through AFM and SEM. The surface topography of the samples was analyzed with a multimode atomic force microscope with Nanoscope V Controller (Bruker Corporation, USA). Three areas of 40 µm × 40 µm were studied per sample with a frequency of 50 Hz and the average roughness values (Ra) were determined with NanoScope Analysis 1.4 (Bruker Corporation) software. The surface morphology was examined with a scanning electron microscope HITACHI S-2400 (Hitachi Instruments Inc., Japan) at 18 kV. Previously, the samples were coated with gold and palladium to make them conductive.

The chemical characterization of the coatings was performed by X-ray photoelectron spectroscopy (XPS) analyses. X-ray photoelectron spectra were obtained using a Kratos AXIS Supra system with a hemispherical electron analyzer and a monochromatic AlKα X-ray source (120 W, 15 kV) operating at 1.33 * 10^{-7} Pa of residual pressure. Spectra were collected at 160 eV (survey spectra) and 20 eV (high resolution spectra). Binding energies were related to C1s signal for the adventitious carbon at 285 eV. The results obtained were deconvoluted by means of PeakFit 4.12 (SPSS Inc.). Each sample was analyzed in triplicate.

The wettability of the samples was measured by using the sessile drop method. Five distilled water drops of 10 µl were deposited on each sample type and their static water contact angles (WCA) were measured by digital image analysis using the ImageJ free software (Schneider, Rasband, & Eliceiri, 2012) with the low-bond axisymmetric drop shape analysis plugin (Stalder et al., 2010). The average WCA for each sample was calculated from the analysis of five respective measurements. The lower the WCA of a sample is, the higher its wettability is and the more hydrophilic the sample is.

2.7. Statistical analysis

Statistical analyses were performed by analysis of variance (ANOVA) after normalization by logarithmic transformation of OD_{595} data. Differences were considered statistically significant at $p < 0.05$. During the initial anti-biofilm screening of coatings, biofilm production on coated SS plates (n=4) was compared to biofilm production on uncoated SS plates (n=4) obtained on the same experimental day and also to biofilm production on all the uncoated SS plates analyzed throughout the study (n=56). Coatings were considered as anti-biofilm coatings when the differences between biofilm production on coated and uncoated SS plates were significant in both cases. The Pearson correlation coefficient was calculated to study the linear relationship between the cellular hydrophobicity of the three *L. monocytogenes* strains and their relative biofilm production on the coating AP10+AA6, considering a statistically significant correlation at $p < 0.05$. Statistical analyses were performed with R Studio version 3.5.3.

3. RESULTS

3.1. Anti-biofilm screening of coatings

For the anti-biofilm screening of coatings, biofilm production by *L. monocytogenes* CECT911 and *E. coli* CECT515 on coated plates was analyzed and compared to that on control uncoated SS AISI 316. **Figure 2** shows the relative biofilm production levels obtained for the 20 tested coatings. In a first step of coatings optimization, coatings made of only one type of precursor (TEOS or AA) were applied with different number of passes and modifying various APPJ parameters (**Figure 2(A,B)**). Then, coatings consisting of a base coating and a functional coating, both of them made of different precursors and applied modifying various APPJ parameters, were tested (**Figure 2(C,D)**). Among those coatings showing anti-biofilm activity (i.e., relative biofilm productions <100%), the best results were obtained for *L. monocytogenes* and, in particular, for two coatings consisting of a base coating of APTES and a functional coating of TEOS (AP10+TE6) or acrylic acid (AP10+AA6). For these two coatings the relative biofilm production obtained was 55% and 26%,

respectively. These two coatings were the ones selected for further characterization. Also, for additional tests, a new coating was introduced which modified the most efficient one through the replacement of acrylic acid with succinic acid (AP10+SA6). Since acrylic acid (CH_2=CH-COOH) gave promising results when it was used for the deposition of a functional coating over a base coating of APTES (AP10+AA6), we decided to test another precursor of similar chemical nature that could provide a functional coating with the same type of functional groups as those of acrylic acid. Therefore, succinic acid (HOOC-$(CH_2)_2$-COOH) was introduced to test the hypothesis of whether its higher content on carboxylic groups could increase the anti-biofilm activity of the coating. On the other hand, the results that were obtained in the screening with *E. coli* suggested that the coatings were not sufficiently effective against it. Most of the coatings showed a pro-biofilm activity with *E. coli* (i.e., relative biofilm productions >100%) and only the coating TE10, with a relative biofilm production of 31%, showed a considerable anti-biofilm activity. Given the overall inefficacy of the coatings against biofilm production by *E. coli*, this bacterial species was not considered for further analysis.

The anti-biofilm activity of the three selected coatings (AP10+TE6; AP10+AA6; AP10+SA6) was subsequently assessed for three *L. monocytogenes* strains under four biofilm development conditions: 37 °C / 24 hours, 37 °C / 48 hours, 12 °C / 144 hours and 12 °C / 288 hours (**Figure 3**). Additionally to the incubation conditions used in the initial screening process, a lower temperature of 12 °C with longer incubation times was included as a more accurate representation of the conditions prevailing during food processing. Remarkably, the greatest anti-biofilm activity was achieved at 12 °C, with the differences in biofilm production between coated and uncoated samples being statistically significant at this temperature for all of the three strains on the coating AP10+AA6 (**Figure 3**, row 2). Indeed, relative biofilm productions observed at 12 °C ranged from 10 to 24 % on this coating, while at 37 °C the relative biofilm productions ranged between 34 and 177 %. The results of biofilm formation inhibition obtained through the crystal violet assay were corroborated through the visualization by SEM of the biofilms formed by *L. monocytogenes* CECT911 on the coated and uncoated SS plates. The images in **Figure 4** show a visible decrease in biofilm formation on the AP10+AA6 (**Figure 4**, column C) coating when compared with that observed on uncoated SS plates, especially for biofilms developed at 12 °C. Considering the differences observed in anti-biofilm activity depending on the biofilm development conditions (time and temperature), the cellular hydrophobicity of the three *L. monocytogenes* strains was measured after their incubation for 24 hours at 37 °C and 144 hours at 12 °C. The three strains showed a reduction in the adherence to hydrocarbons when they were grown at 12 °C, which was particularly marked for *L. monocytogenes* ULE1264 (**Figure 5**). In the **Figure 5** it is also possible to appreciate that cellular hydrophobicity was positively correlated (Pearson correlation coefficient of 0.967; p = 0.0017) with relative biofilm production levels on the coating AP10+AA6.

3.2. Morphological and physico-chemical characterization of the coatings

The surface morphology of the three selected coatings (AP10+TE6, AP10+AA6, AP10+SA6), the uncoated SS plates, and the base coating of APTES were studied by AFM and SEM (**Figure 6**). With both approaches it was possible to appreciate how the characteristic grooves of SS (**Figure 6(A)**) were smoothed by the application of the different coatings, although no major effects in the calculated average roughness values were observed. The coatings AP10+TE6 (**Figure 6(C)**) and AP10+SA6 (**Figure 6(E)**) showed a lumpy surface, similar to that of the base coating AP10 (**Figure 6(B)**). On the other hand, the coating AP10+AA6 (**Figure 6(D)**) showed a smoother surface and the lowest surface roughness.

The chemical composition of uncoated and coated SS plates was determined by XPS analysis. C1s spectra were deconvoluted in order to quantify the relative abundance of C-C/C-H, C-O, C=O and O-C=O groups (**Figure 7**) with the component at approximately 285 eV corresponding to C-C and C-H bonds, the component at 286.5 - 287.2 eV corresponding to C-O bonds, and the component at 288.5 - 289.4 eV corresponding to O-C=O bonds. It is noticeable that the spectra of the coating AP10+AA6 (**Figure 7(D)**), which was the coating with the highest anti-biofilm activity, showed a component corresponding to O-C=O bonds much stronger than the other coatings. **Table 2** gathers the main results of the XPS analysis providing the atomic percentages of C, O, N, Si, Fe and Cr; and the total contribution of polar groups (C-O, C=O and O-C=O) in the C1s spectra. The presence of Fe and Cr is characteristic for SS AISI 316 materials. As expected, Fe and Cr were not detected on the coated samples, which is due to the fact that the XPS analysis only reaches a depth of 10 nm. These results evidence that SS AISI 316 plates were successfully covered by the coatings. The high atomic percentage of Si on the base coating AP10 and the functional coating AP10+TE6 can be explained by the presence of Si in the composition of both precursors (i.e., APTES and TEOS). The fact that the greatest percentage of N was measured in the base coating AP10 is due to the presence of this element in the amine groups of the APTES molecule. The lower percentage of N and the considerably greater percentage of O in the coating AP10+TE6, in comparison with those of the base coating AP10, suggest that the base coating of APTES was successfully covered by the functional coating of TEOS. Although TEOS does not contain nitrogen, the low atomic N content in the coating AP10+TE6 could come from the N_2 used for the plasma generation. Also, the almost null atomic percentage of Si in the coating AP10+AA6 indicates that the AP10 base coating was sufficiently covered by the AA coating. Regarding the atomic percentages measured for the coating AP10+SA6, they suggest that the base coating of APTES was not fully covered by the SA coating. On the one hand, the lower percentages of C and N and the greater percentage of O in the coating AP10+SA6 than in the coating AP10 suggest the incorporation of SA in the functional coating. On the other hand, the unexpected high percentage of Si in the AP10+SA6 coating suggests that its surface still exhibited the base coating AP10 to a notable extent because, in this case, the only source of Si was the APTES precursor used for the base coating.

The wettability of uncoated and coated SS plates was measured through the determination of the WCA (**Table 2**). In general, the wettability was higher (i.e., the WCA was lower) on the coated samples than on the uncoated SS plates (WCA = 89.45°). The WCA was especially low in the case of the AP10+AA6 coating (WCA = 18.74°), the one that showed the best results in the anti-biofilm activity assays.

4. DISCUSSION

Biofilm formation on surfaces and equipment in the food industry can lead to cross contamination of food products with associated health risks for consumers and important economic losses for food business operators. That is why great research effort is being devoted on developing modified surfaces that limit or reduce the formation of biofilms through different strategies. Several studies have reported the anti-biofilm efficacy of different types of coatings applied on stainless steel (Cao et al., 2018; Faure et al., 2012; Friedlander et al., 2019; Zhong et al., 2013), a commonly used material in food processing facilities, including the equipment (Dürr, 2007). According to the literature, functional coatings that reduce biofilm formation can be classified into (1) coatings that contain and release biocidal agents, (2) coatings with immobilized antimicrobial agents on their surface and (3) coatings that modify the surface physico-chemical properties in a way that microbial attachment is minimized (Cattò et al., 2018; Múgica-Vidal et al., 2019; Sardella et al., 2016). The application of coatings that modify the physico-chemical properties of food contact surfaces is particularly promising because it can prevent the first step of biofilm formation (i.e., microbial attachment) and avoids using biocidal agents, thus being able to produce non-toxic surfaces with antibacterial effects. This study is focused on the development of anti-biofilm coatings applied by Non-Equilibrium Atmospheric Plasma, a coating deposition technology with numerous advantages that facilitate its scalability at industrial level.

In the initial screening, coatings AP10+AA6 and AP10+TE6 were among the most promising coatings given their anti-biofilm activity against *L. monocytogenes*. These two composed coatings, which had a base coating of APTES, were selected for further characterization as this material contains siloxane, which provides a higher mechanical resistance to the coating, and amines, which promote its adhesion to the surface (Múgica-Vidal, Alba-Elías, Sainz-García, & Ordieres-Meré, 2014; Sainz-García, Alba-Elías, Múgica-Vidal, & Pantoja-Ruiz, 2016). Furthermore, the base coating of APTES was able to modify the surface morphology of the plates in a way that the characteristic grooves of the SS became less evident, as shown by the results of the morphological characterization. Since grooves are potential shelters where microorganisms have a greater contact area that promotes microbial adhesion (Lorenzetti et al., 2015; Medilanski, Kaufmann, Wick, Wanner, & Harms, 2002; Wu, Zhang, Liu, Suo, & Li, 2018), the morphological modification that is provided by the base coating of APTES (AP10) was considered as a convenient starting point for the subsequent deposition of a functional coating using a different precursor. In addition, a new variation was introduced for the coating with the best anti-biofilm potential by using the same base coating of APTES and replacing AA by SA in the functional coating (AP10+SA6). SA, a dicarboxylic acid, was selected

as a replacement of AA, a monocarboxylic acid, due to the antibacterial properties attributed to carboxylic groups (Ping et al., 2011). Also, SA has been previously used for food decontamination (Purohit & Mohan, 2019; Radkowski, Zdrodowska, & Gomółka-Pawlicka, 2018; Wang et al., 2019) and in edible films with antimicrobial properties (Cheng, Wang, & Weng, 2015). These selected coatings were subjected to a second stage of anti-biofilm assays that were conducted not only at 37 ^{o}C but also at 12 ^{o}C, which is the maximum ambient temperature recommended by the European Parliament and the Council of the European Union in facilities processing products of animal origin (Regulation 853/2004/EC). This latter incubation temperature resulted in an increased anti-biofilm activity for the coating AP10+AA6, both after 6 and 288 hours of incubation. According to the results of the anti-biofilm assays (**Figure 3**), the most effective of the three coatings thoroughly characterized was the coating AP10+AA6. The ineffectiveness of this coating after incubation at 37 ^{o}C for 48 hours may be because its surface topography is smoother than that of the uncoated SS. It has been previously observed that a delay in biofilm formation can occur on smooth surfaces, thus causing an asynchrony of the attachment and detachment processes that are involved in biofilm development in comparison with rougher surfaces (Mosquera-Fernández, Rodríguez-López, Cabo, & Balsa-Canto, 2014).

Several surface properties, including roughness, wettability and physico-chemical composition, have been reported to play a role in the complex mechanism of microbial adhesion to surfaces (Trentin et al., 2014; Yuan, Hays, Hardwidge, & Kim, 2017). The analysis of the surface topography through AFM and SEM suggests that smoother surfaces, like those of the coating AP10+AA6 (with the lowest roughness value), can help to limit adhesion and biofilm formation by *L. monocytogenes*. The application of the coatings reduced the occurrence of grooves in the stainless steel, although mean roughness values (Ra) did not totally reflect the topographic changes visually observed in the AFM and SEM images. On the uncoated stainless steel, microorganisms may be more protected in grooves and have a higher contact area which can result in an increased adhesion (Lorenzetti et al., 2015; Medilanski et al., 2002; Wu et al., 2018). However, the different anti-biofilm properties of the selected coatings could not be explained exclusively by their morphology. The wettability of a coating is also an important factor to consider, as extremely hydrophobic or hydrophilic surfaces have been reported to reduce microbial adhesion (Yuan et al., 2017). The low WCA of the most effective anti-biofilm coating, i.e. AP10+AA6 (WCA=18.74^{o}), indicates that this coating has a strong hydrophilic character. This suggests that the formation of a hydration layer is what prevents the adherence of *L. monocytogenes* (**Figure 8**). It has been previously proposed that the formation of a layer of water molecules tightly bound to the surface through hydrogen bonds creates a physical and energetic barrier which limits the interaction between bacterial proteins and the surface (Bazaka et al., 2015; Oh et al., 2018; Peng, Song, & Fort, 2006; Sardella et al., 2016; Yuan et al., 2017). When surface hydration is strong, the water barrier mechanism can prevent the direct contact between the proteins and the surface (Zheng et al., 2005), thus avoiding the initial formation of a conditioning film that would have subsequently promoted bacterial adhesion. Therefore, this mechanism is able to prevent biofilm formation in its earliest stages. The

XPS chemical characterization and wettability results suggest that the increased abundance of oxygen polar groups (C-O, C=O, O-C=O) is associated with an increase in surface hydrophilicity and therefore a reduction in the WCA. These functional groups, and especially the carboxyl groups (COOH), have a polar character that can explain the hydrophilic nature of the anti-biofilm coatings (Park et al., 2019; Sönmez, Fazeli Jadidi, Kazmanli, Birer, & Ürgen, 2016; Vandencasteele & Reniers, 2010). However, despite SA is a dicarboxylic acid and AA is a monocarboxylic acid, an increase in the abundance of carboxyl groups in the AP10+SA6 coating, as compared to the AP10+AA6 coating, was not observed.

Overall, a relationship existed between the abundance of total polar groups, the wettability of the coatings and their anti-biofilm activity. It is noticeable that the coating with more total polar groups (54.64%) was AP10+AA6, which was also the one with the lowest WCA (18.74°) and the greatest anti-biofilm activity, while uncoated SS plates showed the lowest content in total polar groups (29.81%) and the highest WCA (89.45°). These findings are in agreement with recent work conducted by the authors, which reported the anti-biofilm effects of atmospheric-pressure plasma-polymerization of AA on 3D-printed substrates against *L. monocytogenes*, *E. coli* and *P. aeruginosa* (Muro-Fraguas et al., 2020). However, the topography of the surface may be also relevant for the anti-biofilm activity obtained, since the roughness analysis suggested that a smoother surface also promoted a decrease in biofilm development. As observed by Mosquera-Fernández et al. (2014) in their characterization of the temporal evolution of *L. monocytogenes* biofilms on SS surfaces, topographical features like the grooves of the uncoated SS of the present work (**Figure 6(A)**) can promote the entrapment and accumulation of *L. monocytogenes* cells within them during early biofilm development, probably because of the increased microorganism-surface contact area, and facilitate the formation of microcolonies. Topographical features may also affect the cleanability of the surface by protecting the retained cells from removal and facilitating biofilm regrowth (Verran, Rowe, & Boyd, 2001). After surface cleaning, the bacterial cells that are retained inside the grooves can be reached by disinfectant residues and undergo tolerance phenomena. On the other hand, a smoother surface without grooves like that of coating AP10+AA6 (**Figure 6(D)**) could prevent the aforementioned problems, thus leading to less biofilm development. It is also important to bear in mind that microbial attachment is a complex process influenced in a significant manner by environmental conditions such as temperature (Abdallah et al., 2019; Lee, Hébraud, & Bernardi, 2017). Abdallah et al. (2014) observed that the hydrophobicity of *P. aeruginosa* and *S. aureus*, which was measured through their affinity to hexadecane, and their adhesion onto SS increased when the growth temperature increased. Di Bonaventura et al. (2008) measured higher hydrophobicity level of *L. monocytogenes* strains and higher biofilm formation on polystyrene, glass and SS surfaces at 37 °C than at lower temperatures. SEM imaging also revealed that *L.monocytogenes* biofilm development was affected by the growth temperature. Whereas at 22 °C and 37 °C the biofilm exhibited a complex organization, at 4 °C and 12 °C it consisted only of sparse aggregations of cells and low amounts of extracellular polymeric substances. These observations are in agreement with the results of the present work, where lower hydrophobicity and lower relative biofilm production were

observed at 12 °C than at 37 °C for the three *L. monocytogenes* strains (**Figure 5**). Also, as shown in the SEM images of **Figure 4**, lower biofilm formation was observed after incubation at 12 °C (**Figure 4**, row 2) than at 37 °C (**Figure 4**, row 1) on the uncoated SS and on the coatings. These facts suggest that the reduction of the incubation temperature from 37 °C to 12 °C may have affected the *L. monocytogenes* strains making them less prone to adhere to the SS plates. Additionally, bacterial adhesion would have been further impaired by the formation of a hydration layer on the strongly hydrophilic coating AP10+AA6. The combination of these two factors (i.e., the changes in bacterial hydrophobicity at low temperatures and the strongly hydrophilic nature of the coated surface) may be the cause of the low relative biofilm productions obtained for the three *L. monocytogenes* strains at 12°C on the coating AP10+AA6.

5. CONCLUSIONS

In this study, anti-biofilm coatings that modified the physicochemical properties of stainless steel surfaces were successfully developed by using Non-Equilibrium Atmospheric Plasma. The characterization of the coatings suggested that their anti-biofilm effects against *L. monocytogenes* is due to a reduction in bacterial attachment that can be explained by the following findings:

- The hydrophilic character of the coatings that can be a result of the increased abundance of oxygen polar groups (C-O, C=O and especially O-C=O), which suggested that a hydration layer might have acted as a water barrier against bacterial cells and proteins.
- A reduction in the occurrence of grooves of the SS substrate, which can reduce the entrapment of bacterial cells in zones with high cell-surface contact area.

This mode of action allows the development of non-toxic surfaces with antibacterial effects, which would make these coatings advantageous over other approaches like those that use biocidal agents.

Also, an influence of the incubation temperature on *L. monocytogenes* cellular hydrophobicity and biofilm formation has been identified. These bacteria are less hydrophobic and seem less prone to adhere to the studied surfaces at 12 °C than at 37 °C, thus leading to lower biofilm production.

Coating AP10+AA6 showed the most promising results against *L. monocytogenes* strains in this study, especially after incubation at 12 °C. The increased effectiveness coating AP10+AA6 at this relatively low temperature, representative of the conditions prevailing during food processing, would facilitate its implementation in the food industry. Considering all the aforementioned, *L. monocytogenes* biofilm formation on SS under incubation conditions that are similar to those of real food-processing environments has been reduced by 90% through the plasma-polymerization of coating AP10+AA6. These results will be able to be incorporated to the arsenal of strategies available for the control of biofilms of pathogenic bacteria in the food industry.

Further experiments evaluating the durability and toxicity of the coatings are needed to ensure the usability and safety of the developed coatings in food-related settings. Also, in order to check that the anti-biofilm activity of these coatings is not limited only to *L. monocytogenes*, tests with other microorganisms are needed. Furthermore, considering the fact that several pathogenic microorganisms usually coexist in food-processing environments, future work will characterize the effectivity of the coatings on mixed-species biofilms to validate the usefulness of this technology in realistic settings. To better understand the temporal evolution of biofilm development on the coatings, more incubation times ranging from 24 to 288 hours will also be included for incubation at both 12 ^{o}C and 37 ^{o}C in future work.

ACKNOWLEDGMENTS

This work was supported by Ministerio de Economía, Industria y Competitividad from Spain (MINECO) (project AGL2017-82779-C2-R "Programa Estatal de I+D+i Orientada a los Retos de la Sociedad") and co-funded by the European Regional Development Fund (FEDER) "A way to make Europe".

XPS tests were conducted by the Advanced Microscopy Laboratory (LMA) of The Institute of Nanosciences of Aragon (INA), University of Zaragoza. The authors are thankful to the LMA-INA for the access to their equipment and their expertise.

The AFM images were taken by the Central Research Support Service (SCAI) of the University of Málaga (UMA).

P. Fernández-Gómez is grateful to Junta de Castilla y León and the European Social Fund (ESF) for awarding her a pre-doctoral grant (BOCYL-D-15122017-4). The author E. Sainz-García, as postdoctoral researcher of the University of La Rioja, thanks the postdoctoral training program that is funded by the Plan Propio of the University of La Rioja. The author I. Muro-Fraguas thanks the program of pre-doctoral contracts for the training of research staff funded by the University of La Rioja.

REFERENCES

Abdallah, M., Benoliel, C., Jama, C., Drider, D., Dhulster, P., & Chihib, N. E. (2014). Thermodynamic prediction of growth temperature dependence in the adhesion of *Pseudomonas aeruginosa* and *Staphylococcus aureus* to stainless steel and polycarbonate. *Journal of Food Protection*, *77*(7), 1116–1126. https://doi.org/10.4315/0362-028X.JFP-13-365

Abdallah, M., Mourad, R., Khelissa, S. O., Jama, C., Abozid, M., Drider, D., & Chihib, N. E. (2019). Impact of growth temperature on the adhesion of colistin-resistant *Escherichia* coli strains isolated from pigs to food-contact-surfaces. *Archives of Microbiology*, *201*, 679–690. https://doi.org/10.1007/s00203-019-01632-0

Alvarez-Ordóñez, A., Coughlan, L. M., Briandet, R., & Cotter, P. D. (2019). Biofilms in food processing environments: challenges and opportunities. *Annual Review of Food Science and Technology*, *25*(10), 173–195. https://doi.org/10.1146/annurev-food-032818-121805

Bazaka, K., Jacob, M. V., Chrzanowski, W., & Ostrikov, K. (2015). Anti-bacterial surfaces: Natural agents, mechanisms of action, and plasma surface modification. *RSC Advances*, *5*(60), 48739–48759. https://doi.org/10.1039/c4ra17244b

Cao, P., Li, W. W., Morris, A. R., Horrocks, P. D., Yuan, C. Q., & Yang, Y. (2018). Investigation of the antibiofilm capacity of peptide-modified stainless steel. *Royal Society Open Science*, *5*(3), 172165. https://doi.org/10.1098/rsos.172165

Cattò, C., Villa, F., & Cappitelli, F. (2018). Recent progress in bio-inspired biofilm-resistant polymeric surfaces. *Critical Reviews in Microbiology*, *44*(5), 633–652. https://doi.org/10.1080/1040841X.2018.1489369

Cheng, S. Y., Wang, B. J., & Weng, Y. M. (2015). Antioxidant and antimicrobial edible zein/chitosan composite films fabricated by incorporation of phenolic compounds and dicarboxylic acids. *LWT - Food Science and Technology*, *63*(1), 115–121. https://doi.org/10.1016/j.lwt.2015.03.030

Colagiorgi, A., Bruini, I., Di Ciccio, P. A., Zanardi, E., Ghidini, S., & Ianieri, A. (2017). *Listeria monocytogenes* biofilms in the wonderland of food industry. *Pathogens*, *6*(3), 41. https://doi.org/10.3390/pathogens6030041

Coughlan, L. M., Cotter, P. D., Hill, C., & Alvarez-Ordóñez, A. (2016). New weapons to fight old enemies: Novel strategies for the (bio)control of bacterial biofilms in the food industry. *Frontiers in Microbiology*, *7*, 1641. https://doi.org/10.3389/fmicb.2016.01641

Da Ponte, G., Sardella, E., Fanelli, F., Van Hoeck, A., D'Agostino, R., Paulussen, S., & Favia, P. (2011). Atmospheric pressure plasma deposition of organic films of biomedical interest. *Surface and Coatings Technology*, *205*, S525–S528. https://doi.org/10.1016/j.surfcoat.2011.03.112

Da Ponte, Gabriella, Sardella, E., Fanelli, F., dAgostino, R., Gristina, R., & Favia, P. (2012). Plasma deposition of PEO-like coatings with aerosol-assisted dielectric barrier discharges. *Plasma Processes and Polymers*, *9*, 1176–1183. https://doi.org/10.1002/ppap.201100201

Di Bonaventura, G., Piccolomini, R., Paludi, D., D'Orio, V., Vergara, A., Conter, M., & Ianieri, A. (2008). Influence of temperature on biofilm formation by *Listeria monocytogenes* on various food-contact surfaces: Relationship with motility and cell surface hydrophobicity. *Journal of Applied Microbiology*, *104*(6), 1552–1561. https://doi.org/10.1111/j.1365-2672.2007.03688.x

Dürr, H. (2007). Influence of surface roughness and wettability of stainless steel on soil adhesion, cleanability and microbial inactivation. *Food and Bioproducts Processing*, *85*(C1), 49–56. https://doi.org/10.1205/fbp06011

EFSA, & ECDC. (2019). The European Union One Health 2018 Zoonoses Report. *EFSA Journal*, *17*(12), 5926. https://doi.org/10.2903/j.efsa.2019.5926

505 Faure, E., Vreuls, C., Falentin-Daudré, C., Zocchi, G., van de Weerdt, C., Martial, J., … Detrembleur, C. (2012).
506 A green and bio-inspired process to afford durable anti-biofilm properties to stainless steel.
507 *Biofouling*, *28*(7), 719–728. https://doi.org/10.1080/08927014.2012.704366

508 Friedlander, A., Nir, S., Reches, M., & Shemesh, M. (2019). Preventing biofilm formation by dairy-associated
509 bacteria using peptide-coated surfaces. *Frontiers in Microbiology*, *10*, 1405.
510 https://doi.org/10.3389/fmicb.2019.01405

511 Gratzl, G., Paulik, C., Hild, S., Guggenbichler, J. P., & Lackner, M. (2014). Antimicrobial activity of poly(acrylic
512 acid) block copolymers. *Materials Science and Engineering C*, *38*(1), 94–100.
513 https://doi.org/10.1016/j.msec.2014.01.050

514 Günther, F., Scherrer, M., Kaiser, S. J., Derosa, A., & Mutters, N. T. (2016). Comparative testing of
515 disinfectant efficacy on planktonic bacteria and bacterial biofilms using a new assay based on kinetic
516 analysis of metabolic activity, *122*, 625–633. https://doi.org/10.1111/jam.13358

517 Hsu, L. C., Fang, J., Borca-Tasciuc, D. A., Worobo, R. W., & Moraru, C. I. (2013). Effect of micro- and
518 nanoscale topography on the adhesion of bacterial cells to solid surfaces. *Applied and Environmental*
519 *Microbiology*, *79*(8), 2703–2712. https://doi.org/10.1128/AEM.03436-12

520 Langsrud, S., Sidhu, M. S., Heir, E., & Holck, A. L. (2003). Bacterial disinfectant resistance - A challenge for
521 the food industry. *International Biodeterioration and Biodegradation*, *51*(4), 283–290.
522 https://doi.org/10.1016/S0964-8305(03)00039-8

523 Larsen, M. H., Dalmasso, M., Ingmer, H., Langsrud, S., Malakauskas, M., Mader, A., … Jordan, K. (2014).
524 Persistence of foodborne pathogens and their control in primary and secondary food production
525 chains. *Food Control*, *44*, 92–109. https://doi.org/10.1016/j.foodcont.2014.03.039

526 Lee, B. H., Hébraud, M., & Bernardi, T. (2017). Increased adhesion of *Listeria monocytogenes* strains to
527 abiotic surfaces under cold stress. *Frontiers in Microbiology*, *8*, 2221.
528 https://doi.org/10.3389/fmicb.2017.02221

529 Li, L. (2016). *Prevention of biofilm formation on food contact surfaces by nanoscale plasma coatings*.
530 University of Missouri-Columbia. Retrieved from
531 https://mospace.umsystem.edu/xmlui/handle/10355/57594

532 Lorenzetti, M., Dogša, I., Stošicki, T., Stopar, D., Kalin, M., Kobe, S., & Novak, S. (2015). The influence of
533 surface modification on bacterial adhesion to titanium-based substrates. *ACS Applied Materials and*
534 *Interfaces*, *7*(3), 1644–1651. https://doi.org/10.1021/am507148n

535 Ma, Y., Chen, M., Jones, J. E., Ritts, A. C., Yu, Q., & Sun, H. (2012). Inhibition of *Staphylococcus epidermidis*
536 biofilm by trimethylsilane plasma coating. *Antimicrobial Agents and Chemotherapy*, *56*(11), 5923–
537 5937. https://doi.org/10.1128/AAC.01739-12

538 Medilanski, E., Kaufmann, K., Wick, L. Y., Wanner, O., & Harms, H. (2002). Influence of the surface
539 topography of stainless steel on bacterial adhesion. *Biofouling*, *18*(3), 193–203.
540 https://doi.org/10.1080/08927010290011370

541 Mosquera-Fernández, M., Rodríguez-López, P., Cabo, M. L., & Balsa-Canto, E. (2014). Numerical spatio-
542 temporal characterization of *Listeria monocytogenes* biofilms. *International Journal of Food*
543 *Microbiology*, *182–183*, 26–36. https://doi.org/10.1016/j.ijfoodmicro.2014.05.005

544 Múgica-Vidal, R., Alba-Elías, F., Sainz-García, E., & Ordieres-Meré, J. (2014). Atmospheric plasma-
545 polymerization of hydrophobic and wear-resistant coatings on glass substrates. *Surface and Coatings*
546 *Technology*, *259*, 374–385. https://doi.org/10.1016/j.surfcoat.2014.10.067

547 Múgica-Vidal, R., Sainz-García, E., Álvarez-Ordóñez, A., Prieto, M., González-Raurich, M., López, M., … Alba-
548 Elías, F. (2019). Production of antibacterial coatings through atmospheric pressure plasma: a
549 promising alternative for combatting biofilms in the food industry. *Food and Bioprocess Technology*,

12, 1251–1263. https://doi.org/10.1007/s11947-019-02293-z

Muro-Fraguas, I., Sainz-García, A., Fernández Gómez, P., López, M., Múgica-Vidal, R., Sainz-García, E., … Alba-Elías, F. (2020). Atmospheric pressure cold plasma anti-biofilm coatings for 3D printed food tools. *Innovative Food Science and Emerging Technologies*, *64*, 102404. https://doi.org/10.1016/j.ifset.2020.102404

Oh, J. K., Yegin, Y., Yang, F., Zhang, M., Li, J., Huang, S., … Akbulut, M. (2018). The influence of surface chemistry on the kinetics and thermodynamics of bacterial adhesion. *Scientific Reports*, *8*(1), 17247. https://doi.org/10.1038/s41598-018-35343-1

Pan, Y., Breidt, F., & Kathariou, S. (2006). Resistance of *Listeria monocytogenes* biofilms to sanitizing agents in a simulated food processing environment. *Applied and Environmental Microbiology*, *72*(12), 7711–7717. https://doi.org/10.1128/AEM.01065-06

Park, C. S., Jung, E. Y., Jang, H. J., Bae, G. T., Shin, B. J., & Tae, H. S. (2019). Synthesis and properties of plasma-polymerized methyl methacrylate via the atmospheric pressure plasma polymerization technique. *Polymers*, *11*(3), 396. https://doi.org/10.3390/polym11030396

Peng, C., Song, S., & Fort, T. (2006). Study of hydration layers near a hydrophilic surface in water through AFM imaging. *Surface and Interface Analysis*, *38*, 975–980. https://doi.org/10.1002/sia.2368

Ping, X., Wang, M., & Xuewu, G. (2011). Surface modification of poly(ethylene terephthalate) (PET) film by gamma-ray induced grafting of poly(acrylic acid) and its application in antibacterial hybrid film. *Radiation Physics and Chemistry*, *80*(4), 567–572. https://doi.org/10.1016/j.radphyschem.2010.12.011

Purohit, A., & Mohan, A. (2019). Antimicrobial effects of pyruvic and succinic acids on *Salmonella* survival in ground chicken. *LWT - Food Science and Technology*, *116*, 108596. https://doi.org/10.1016/j.lwt.2019.108596

Radkowski, M., Zdrodowska, B., & Gomółka-Pawlicka, M. (2018). Effect of succinic acid on elimination of *Salmonella* in chicken meat. *Journal of Food Protection*, *81*(9), 1491–1495. https://doi.org/10.4315/0362-028X.JFP-17-446

Regulation 853/2004/EC, 25/06/2004. Regulation (EC) No 853/2004 of the European Parliament and of the Council of 29 April 2004 Laying Down Specific Hygiene Rules for Food of Animal Origin, L226, Brussels, pp. 22-82.

Rodríguez-López, P., Rodríguez-Herrera, J. J., Vázquez-Sánchez, D., & López Cabo, M. (2018). Current knowledge on *Listeria monocytogenes* biofilms in food-related environments: Incidence, resistance to biocides, ecology and biocontrol. *Foods*, *7*(6), 85. https://doi.org/10.3390/foods7060085

Sainz-García, E., Alba-Elías, F., Múgica-Vidal, R., & Pantoja-Ruiz, M. (2016). Promotion of tribological and hydrophobic properties of a coating on TPE substrates by atmospheric plasma-polymerization. *Applied Surface Science*, *371*, 50–60. https://doi.org/10.1016/j.apsusc.2016.02.186

Sardella, E., Palumbo, F., Camporeale, G., & Favia, P. (2016). Non-equilibrium plasma processing for the preparation of antibacterial surfaces. *Materials*, *9*(7), 515. https://doi.org/10.3390/ma9070515

Schneider, C. A., Rasband, W. S., & Eliceiri, K. W. (2012). NIH Image to ImageJ: 25 years of image analysis. *Nature Methods*, *9*(7), 671–675. https://doi.org/10.1038/nmeth.2089

Skowron, K., Wałecka-Zacharska, E., Grudlewska, K., Gajewski, P., Wiktorczyk, N., Wietlicka-Piszcz, M., … Gospodarek-Komkowska, E. (2019). Disinfectant susceptibility of biofilm formed by *Listeria monocytogenes* under selected environmental conditions. *Microorganisms*, *7*(9), 280. https://doi.org/10.3390/microorganisms7090280

Sönmez, T., Fazeli Jadidi, M., Kazmanli, K., Birer, Ö., & Ürgen, M. (2016). Role of different plasma gases on the surface chemistry and wettability of RF plasma treated stainless steel. *Vacuum*, *129*, 63–73. https://doi.org/10.1016/j.vacuum.2016.04.014

595 Stalder, A. F., Melchior, T., Müller, M., Sage, D., Blu, T., & Unser, M. (2010). Low-bond axisymmetric drop
596 shape analysis for surface tension and contact angle measurements of sessile drops. *Colloids and*
597 *Surfaces A: Physicochemical and Engineering Aspects*, *364*(1–3), 72–81.
598 https://doi.org/10.1016/j.colsurfa.2010.04.040

599 Stallard, C. P., McDonnell, K. A., Onayemi, O. D., O'Gara, J. P., & Dowling, D. P. (2012). Evaluation of protein
600 adsorption on atmospheric plasma deposited coatings exhibiting superhydrophilic to
601 superhydrophobic properties. *Biointerphases*, *7*(1–4), 31. https://doi.org/10.1007/s13758-012-0031-0

602 Trentin, D. S., Bonatto, F., Zimmer, K. R., Ribeiro, V. B., Antunes, A. L. S., Barth, A. L., … Macedo, A. J. (2014).
603 N_2/H_2 plasma surface modifications of polystyrene inhibit the adhesion of multidrug resistant bacteria.
604 *Surface and Coatings Technology*, *245*, 84–91. https://doi.org/10.1016/j.surfcoat.2014.02.046

605 Vandencasteele, N., & Reniers, F. (2010). Plasma-modified polymer surfaces: Characterization using XPS.
606 *Journal of Electron Spectroscopy and Related Phenomena*, *178–179*(C), 394–408.
607 https://doi.org/10.1016/j.elspec.2009.12.003

608 Verran, J., Rowe, D. L., & Boyd, R. D. (2001). The effect of nanometer dimension topographical features on
609 the hygienic status of stainless steel. *Journal of Food Protection*, *64*(8), 1183–1187.
610 https://doi.org/10.4315/0362-028X-64.8.1183

611 Villanueva, M. E., Salinas, A., Copello, G. J., & Díaz, L. E. (2014). Point of zero charge as a factor to control
612 biofilm formation of <i>Pseudomonas aeruginosa<i> in sol-gel derivatized aluminum alloy plates.
613 *Surface and Coatings Technology*, *254*, 145–150. https://doi.org/10.1016/j.surfcoat.2014.05.074

614 Wang, J., Tao, D., Wang, S., Li, C., Li, Y., Zheng, F., & Wu, Z. (2019). Disinfection of lettuce using organic
615 acids: An ecological analysis using 16S rRNA sequencing. *RSC Advances*, *9*(30), 17514–17520.
616 https://doi.org/10.1039/c9ra03290h

617 Wu, S., Zhang, B., Liu, Y., Suo, X., & Li, H. (2018). Influence of surface topography on bacterial adhesion: A
618 review. *Biointerphases*, *13*(6), 060801. https://doi.org/10.1116/1.5054057

619 Xu, Y., Jones, J. E., Yu, H., Yu, Q., Christensen, G. D., Chen, M., & Sun, H. (2015). Nanoscale plasma coating
620 inhibits formation of *Staphylococcus aureus* biofilms. *Antimicrobial Agents and Chemotherapy*, *59*(12),
621 7308–7315. https://doi.org/10.1128/AAC.01944-15

622 Yang, J. M., Lin, H. T., Wu, T. H., & Chen, C. C. (2003). Wettability and antibacterial assessment of chitosan
623 containing radiation-induced graft nonwoven fabric of polypropylene-*g*-acrylic acid. *Journal of Applied*
624 *Polymer Science*, *90*(5), 1331–1336. https://doi.org/10.1002/app.12787

625 Yuan, Y., Hays, M. P., Hardwidge, P. R., & Kim, J. (2017). Surface characteristics influencing bacterial
626 adhesion to polymeric substrates. *RSC Advances*, *7*(23), 14254–14261.
627 https://doi.org/10.1039/c7ra01571b

628 Zheng, J., Li, L., Tsao, H. K., Sheng, Y. J., Chen, S., & Jiang, S. (2005). Strong repulsive forces between protein
629 and oligo (ethylene glycol) self-assembled monolayers: A molecular simulation study. *Biophysical*
630 *Journal*, *89*(1), 158–166. https://doi.org/10.1529/biophysj.105.059428

631 Zhong, L. J., Pang, L. Q., Che, L. M., Wu, X. E., & Chen, X. D. (2013). Nafion coated stainless steel for anti-
632 biofilm application. *Colloids and Surfaces B: Biointerfaces*, *111*, 252–256.
633 https://doi.org/10.1016/j.colsurfb.2013.05.039

634

LIST OF FIGURE CAPTIONS

Figure 1. (A) Setup used for the plasma-polymerization treatments, (B) scheme of the plasma-polymerization treatments, (C) close view of the APPJ system and the SS plates during a coating deposition, and (D) shapes of the exit of the atomized precursor: (D1) umbrella and (D2) tube.

Figure 2. Relative biofilm production of (A,C) *E. coli* CECT515 and (B,D) *L. monocytogenes* CECT911 on coatings made of (A,B) only one precursor and (C,D) two precursors after an incubation for 24 hours at 37 ^{o}C. Error bars represent the standard deviation, and asterisks indicate statistically significant differences (*, $p < 0.05$) with the uncoated control in the OD at 595 nm.

Figure 3. Relative biofilm production on SS plates coated with (1) AP10+TE6, (2) AP10+AA6 and (3) AP10+SA6 by the strains of *L. monocytogenes* (A) CECT911, (B) ULE1264 and (C) ULE1265 after their incubation at 37 ^{o}C (for 24 and 48 hours) and 12 ^{o}C (for 144 and 288 hours). Error bars represent the standard deviation, and asterisks indicate statistically significant differences with the uncoated control in the OD at 595 nm (*, $p < 0.05$; **, $p < 0.01$; ***, $p < 0.001$).

Figure 4. Scanning electron microscopy images of (A) uncoated SS AISI 316 plates, and SS AISI 316 plates coated with (B) AP10+TE6, (C) AP10+AA6 and (D) AP10+SA6 colonized by *L. monocytogenes* CECT911 after an incubation of 24 hours at 37 ^{o}C (1), or 144 hours at 12 ^{o}C (2), observed at a magnification of 2000x.

Figure 5. Relative biofilm production on SS plates coated with AP10+AA6 (in black) and cellular hydrophobicity (in grey) of *L. monocytogenes* CECT911, ULE1264 and ULE1265 after their incubation at (A) 37 ^{o}C for 24 hours and (B) 12 ^{o}C for 144 hours. Error bars represent the standard deviation.

Figure 6. AFM images (40x40µm) and SEM images (x2000) of (A) uncoated SS AISI 316 plates, and SS AISI 316 plates coated with (B) AP10, (C) AP10+TE6, (D) AP10+AA6 and (E) AP10+SA6. The calculated average roughness values (Ra) are indicated in the upper right corner of the AFM images.

Figure 7. Deconvolution of C1s spectra for (A) uncoated SS AISI 316 plates, and plates covered with (B) AP10, (C) AP10+TE6, (D) AP10+AA6 and (E) AP10+SA6.

Figure 8. Scheme of the interaction between *L. monocytogenes* and (A) uncoated SS AISI 316 plates, and plates of SS AISI 316 coated with the hydrophilic coatings (B) AP10, (C) AP10+TE6, (D) AP10+AA6 and (E) AP10+SA6, showing different degrees of bacterial repulsion according to the generation of hydration layers on the surfaces.

FIGURES AND TABLES

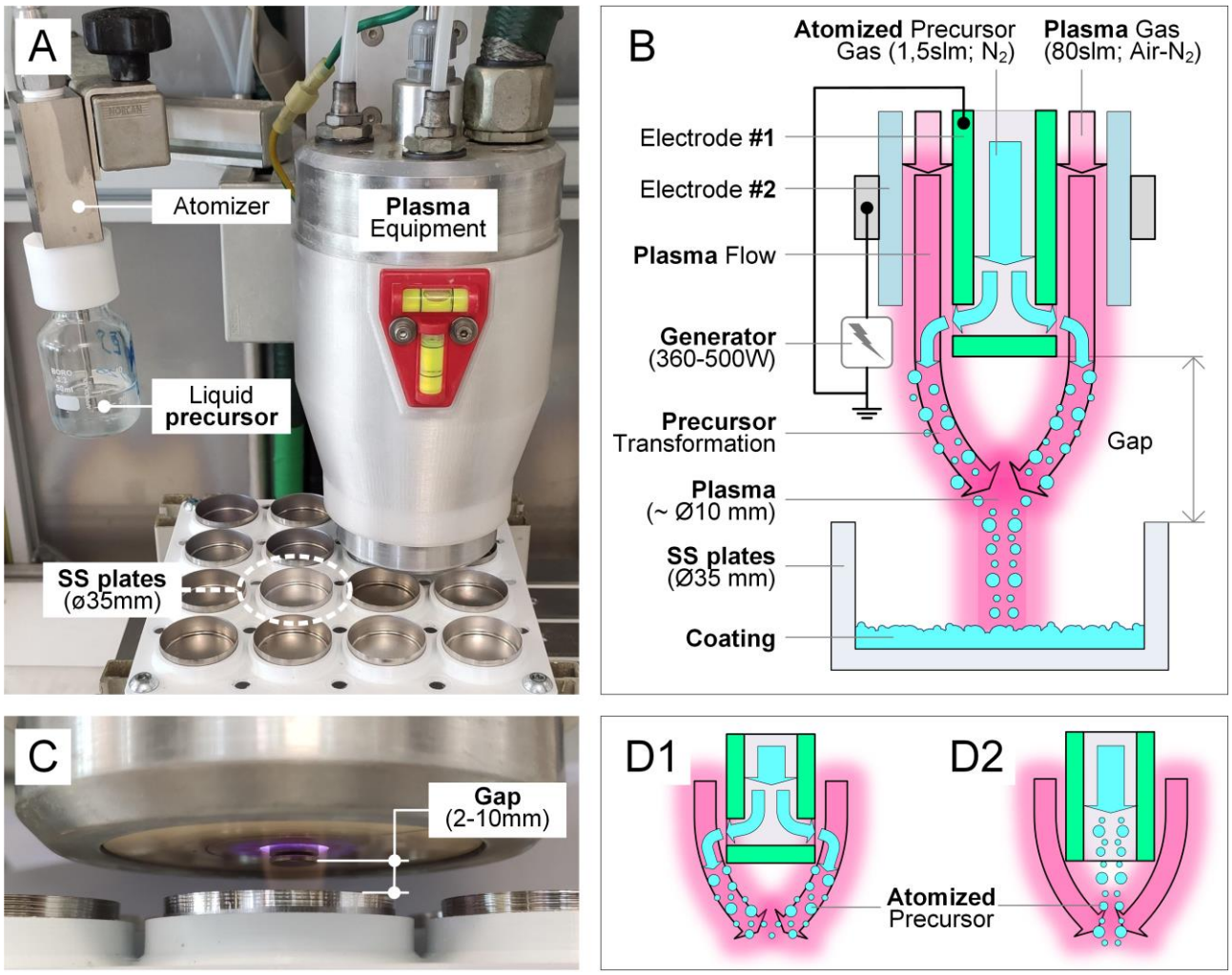

Fig. 1

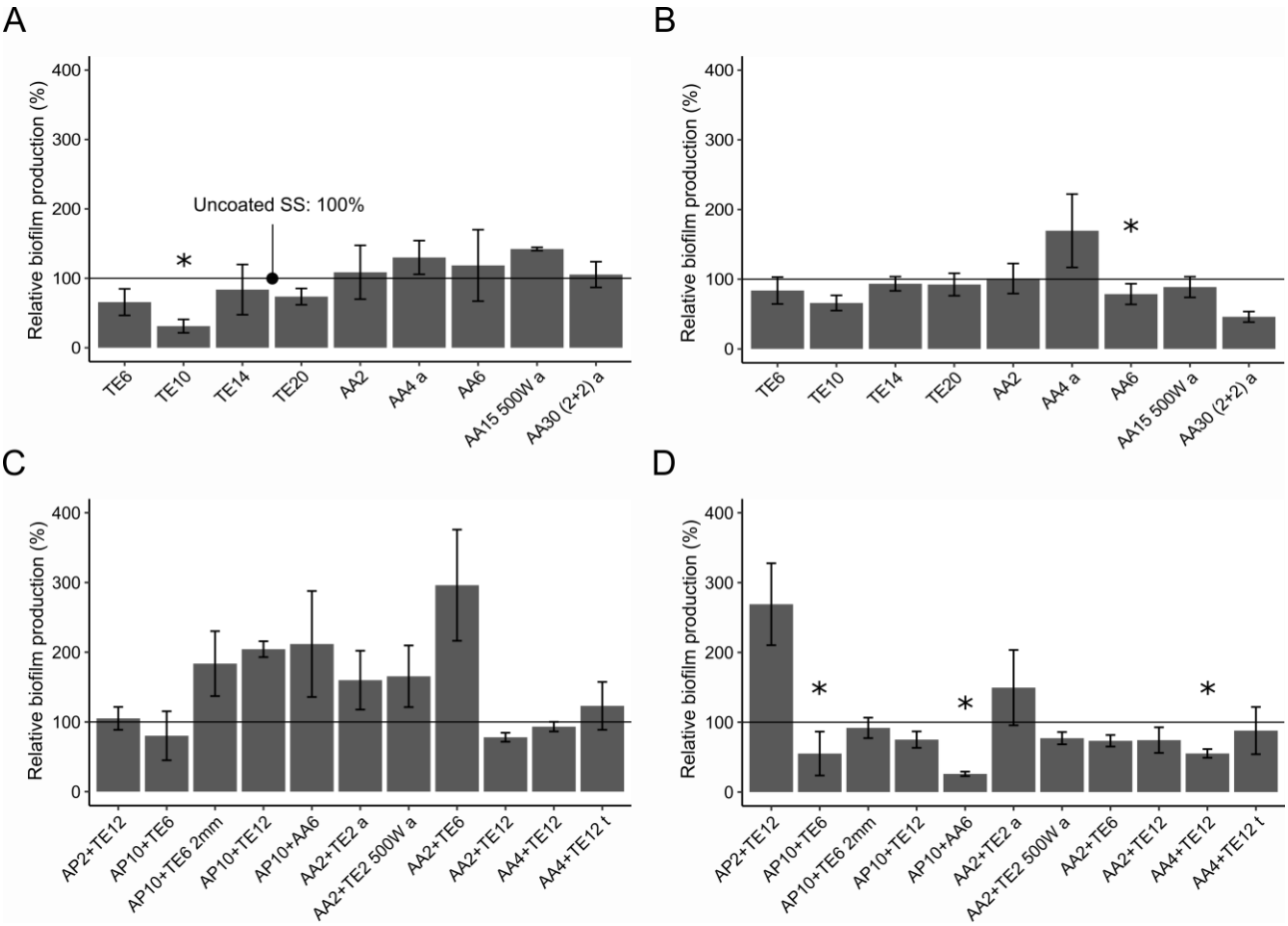
A
B
C
D
Relative biofilm production (%)
Uncoated SS: 100%
TE6
TE10
TE14
TE20
AA2
AA4 a
AA6
AA15 500W a
AA30 (2+2) a
AP2+TE12
AP10+TE6
AP10+TE6 2mm
AP10+TE12
AP10+AA6
AA2+TE2 a
AA2+TE2 500W a
AA2+TE6
AA2+TE12
AA4+TE12
AA4+TE12 t

Fig. 2

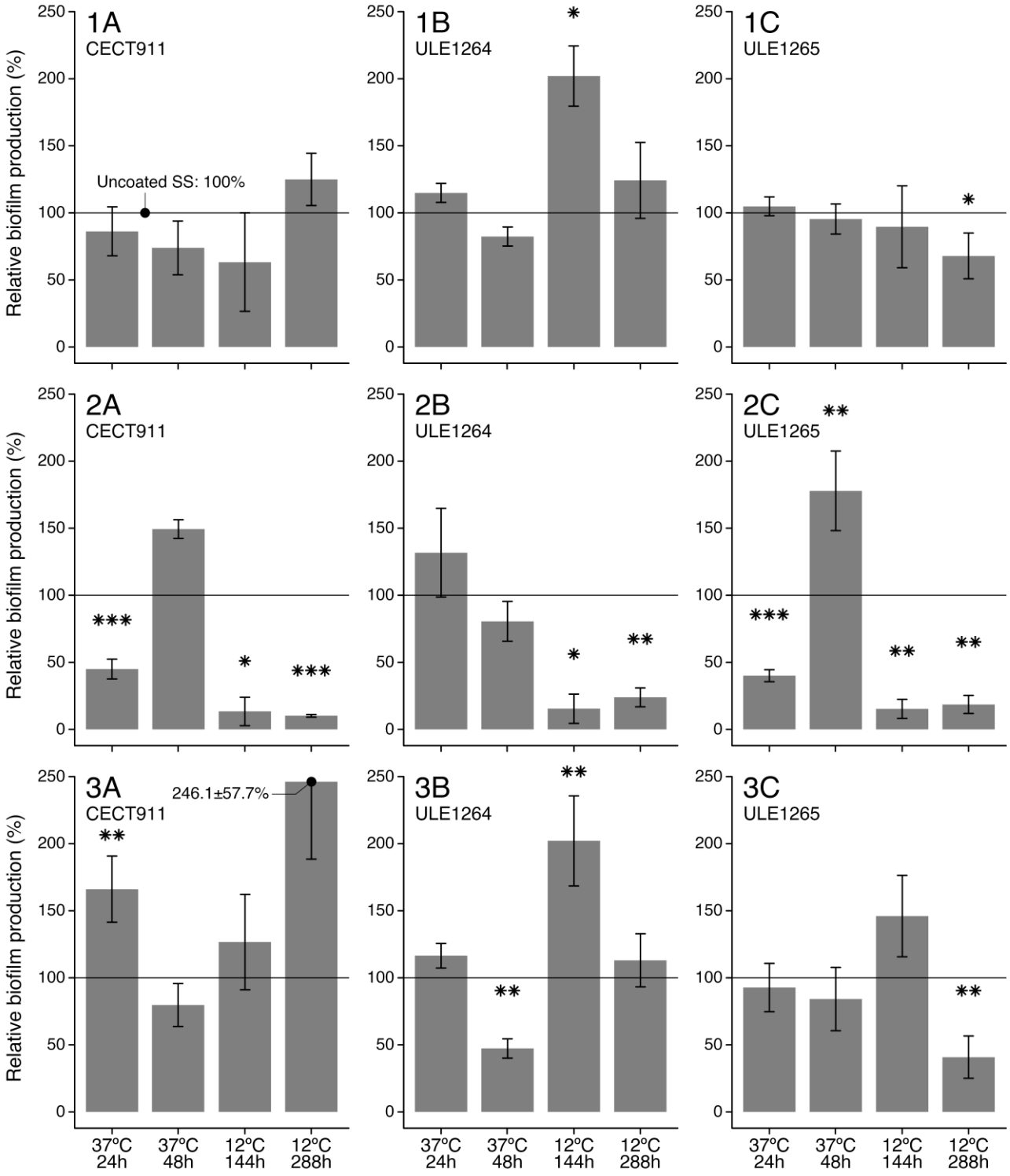
1A
CECT911
Uncoated SS: 100%
1B
ULE1264
1C
ULE1265
2A
CECT911
2B
ULE1264
2C
ULE1265
3A
CECT911
246.1±57.7%
3B
ULE1264
3C
ULE1265
Relative biofilm production (%)
0
50
100
150
200
250
37°C 24h
37°C 48h
12°C 144h
12°C 288h

Fig. 3

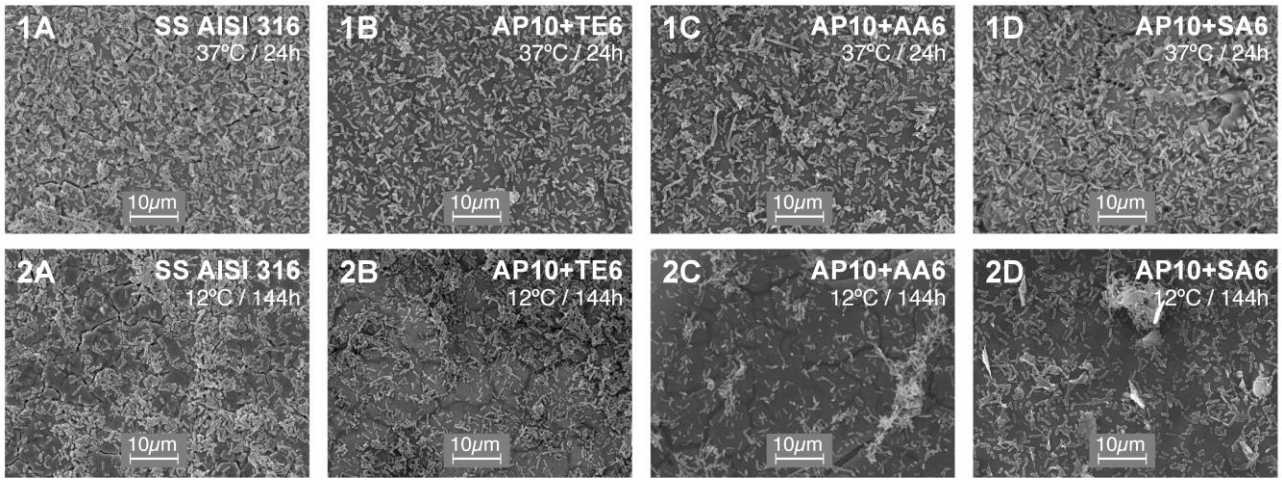
1A
SS AISI 316
37ºC / 24h
1B
AP10+TE6
37ºC / 24h
1C
AP10+AA6
37ºC / 24h
1D
AP10+SA6
37ºC / 24h
2A
SS AISI 316
12ºC / 144h
2B
AP10+TE6
12ºC / 144h
2C
AP10+AA6
12ºC / 144h
2D
AP10+SA6
12ºC / 144h
10μm

Fig. 4

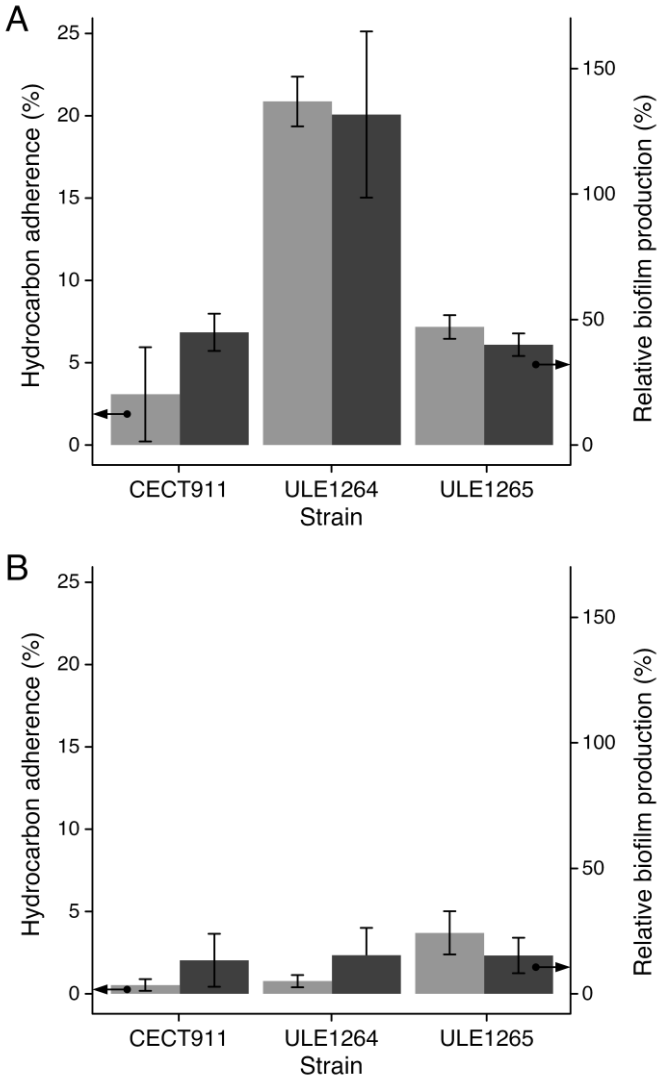
A
B
Hydrocarbon adherence (%)
Relative biofilm production (%)
0
5
10
15
20
25
50
100
150
CECT911
ULE1264
ULE1265
Strain

Fig. 5

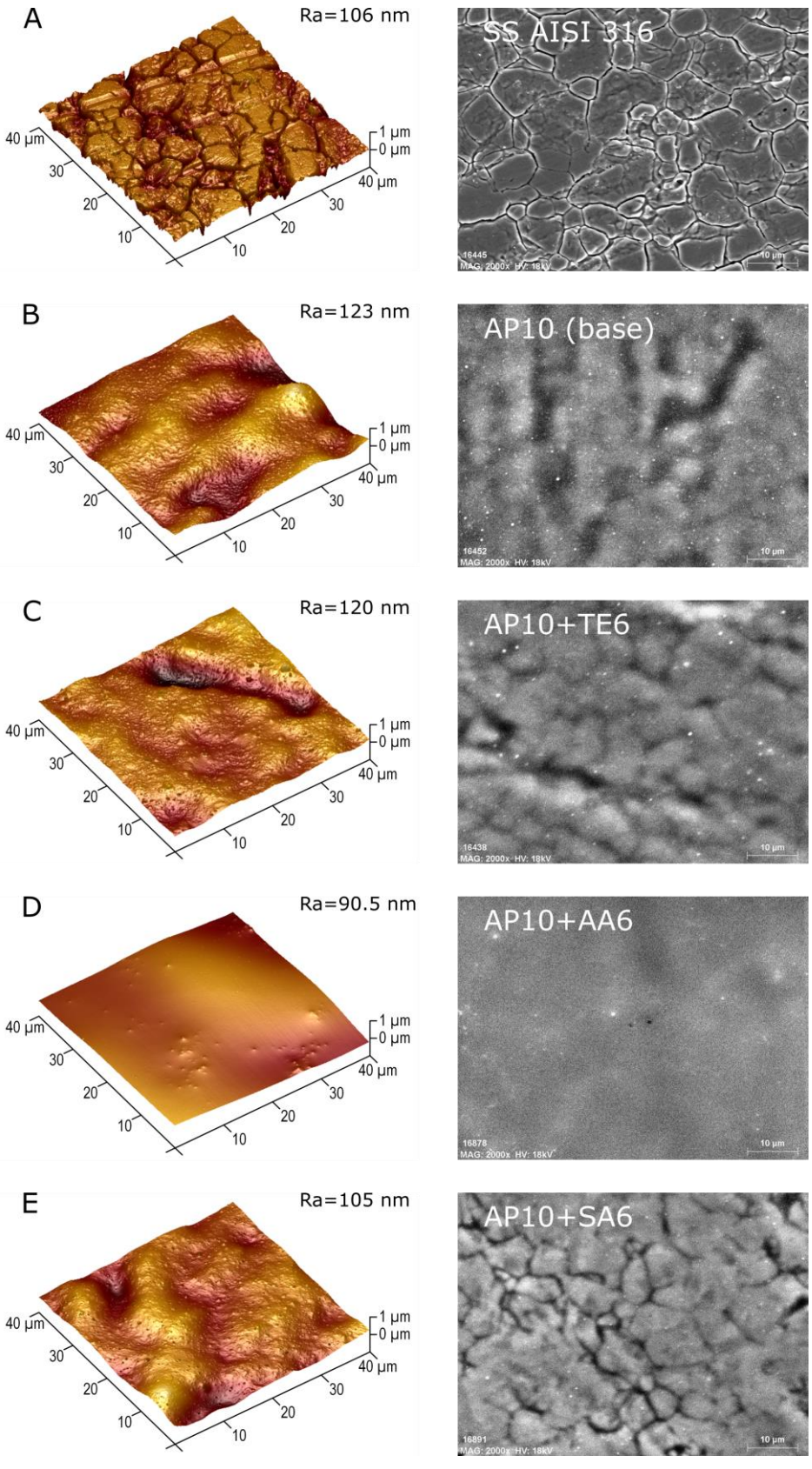
A
Ra=106 nm
SS AISI 316
B
Ra=123 nm
AP10 (base)
C
Ra=120 nm
AP10+TE6
D
Ra=90.5 nm
AP10+AA6
E
Ra=105 nm
AP10+SA6
40 µm
30
20
10
1 µm
0 µm

Fig. 6

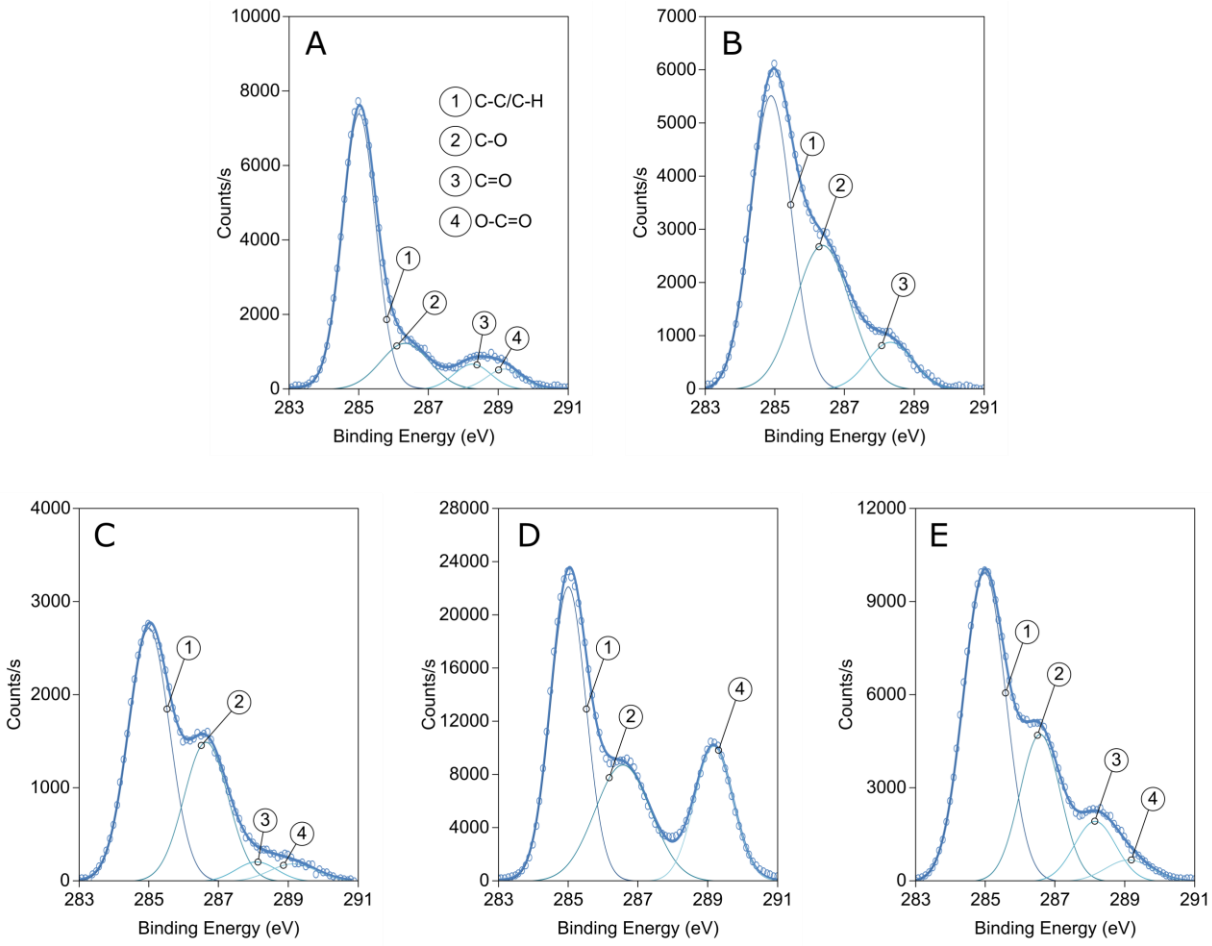

Fig. 7

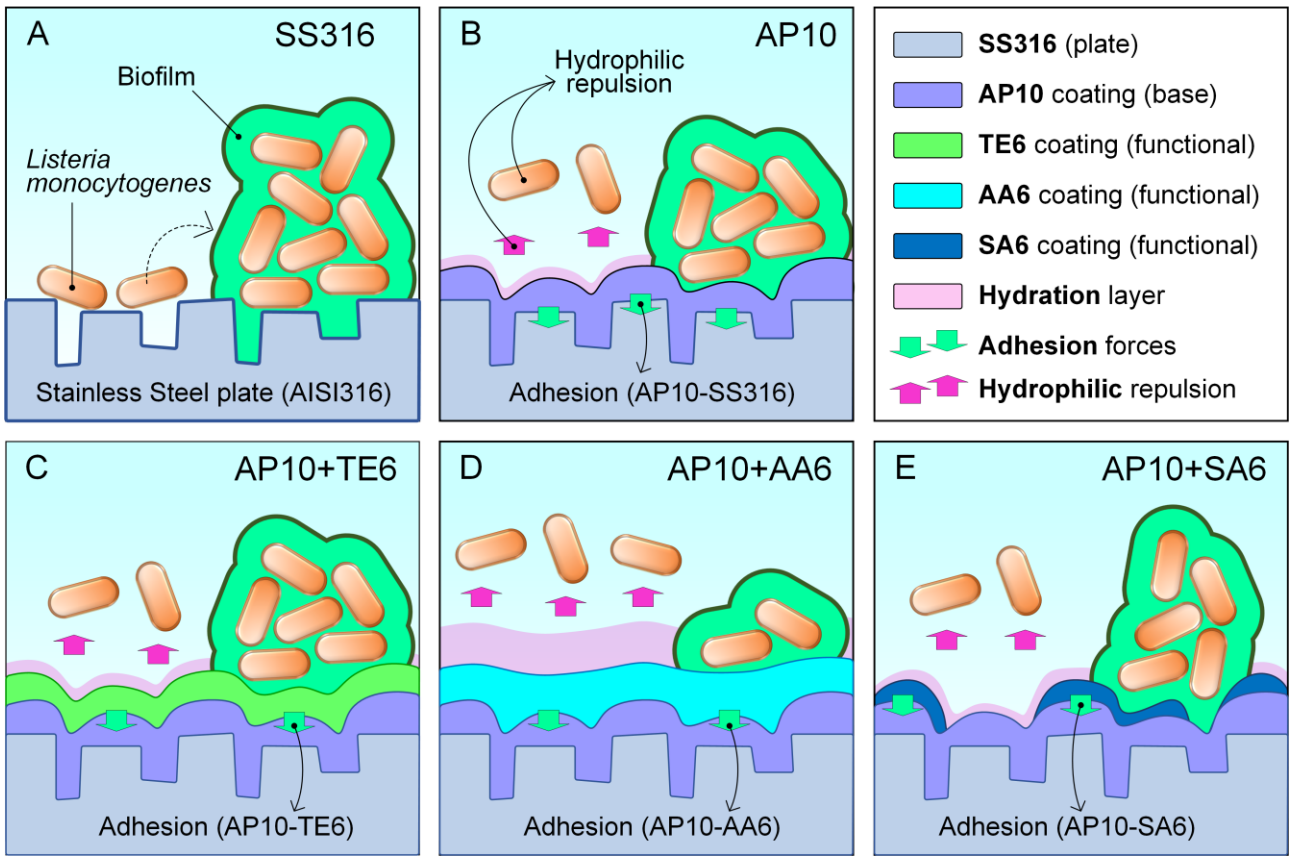
A
SS316
Biofilm
Listeria monocytogenes
Stainless Steel plate (AISI316)
B
AP10
Hydrophilic repulsion
Adhesion (AP10-SS316)
SS316 (plate)
AP10 coating (base)
TE6 coating (functional)
AA6 coating (functional)
SA6 coating (functional)
Hydration layer
Adhesion forces
Hydrophilic repulsion
C
AP10+TE6
Adhesion (AP10-TE6)
D
AP10+AA6
Adhesion (AP10-AA6)
E
AP10+SA6
Adhesion (AP10-SA6)

Fig. 8

Table 1. Coatings tested and Non Equilibrium Atmospheric Plasma processing parameters used.

	Base coating							Functional coating							
Coating code	**Precursor**	**Passes (nº)**	**Plasma gas**	**Precursor gas flow (slm)**	**Gap (mm)**	**Power (W)**	**Speed (mm/s)**	**Precursor**	**Passes (nº)**	**Plasma gas**	**Precursor gas flow (slm)**	**Gap (mm)**	**Power (W)**	**Speed (mm/s)**	**Exit shape**
TE6								TEOS	6	N_2	1.5	10	360	100	Umbrella
TE10								TEOS	10	N_2	1.5	10	360	100	Umbrella
TE14								TEOS	14	N_2	1.5	10	360	100	Umbrella
TE20								TEOS	20	N_2	1.5	10	360	100	Umbrella
AA2								AA	2	N_2	1.5	10	360	100	Umbrella
AA4 a								AA	4	air	1.5	10	360	50	Umbrella
AA6								AA	6	N_2	1.5	10	360	100	Umbrella
AA15 500W a								AA	15	air	1.5	10	500	50	Umbrella
AA30 (2+2) a								AA	30	air	2 + 2	10	360	50	Tube
AP2+TE12	APTES	2	N_2	1.5	10	360	50	TEOS	12	N_2	1.5	10	360	100	Umbrella
AP10+TE6	APTES	10	N_2	1.5	10	360	50	TEOS	6	N_2	1.5	10	360	100	Umbrella
AP10+TE6 2mm	APTES	10	N_2	1.5	2	360	50	TEOS	6	N_2	1.5	2	360	100	Umbrella
AP10+TE12	APTES	10	N_2	1.5	10	360	50	TEOS	12	N_2	1.5	10	360	100	Umbrella
AP10+AA6	APTES	10	N_2	1.5	10	360	50	AA	6	N_2	1.5	10	360	100	Umbrella
AA2+TE2 a	AA	2	air	1.5	10	360	50	TEOS	2	air	1.5	10	360	50	Umbrella
AA2+TE2 500W a	AA	2	air	1.5	10	500	50	TEOS	2	air	1.5	10	500	50	Umbrella
AA2+TE6	AA	2	N_2	1.5	10	360	50	TEOS	6	N_2	1.5	10	360	100	Umbrella
AA2+TE12	AA	2	N_2	1.5	10	360	50	TEOS	12	N_2	1.5	10	360	100	Umbrella
AA4+TE12	AA	4	N_2	1.5	10	360	50	TEOS	12	N_2	1.5	10	360	100	Umbrella
AA4+TE12 t	AA	4	N_2	1.5	10	360	50	TEOS	12	N_2	1.5	10	360	100	Tube

Table 2. Physico-chemical characteristics of uncoated and coated SS plates, as determined through XPS analysis and wettability (WCA) and surface roughness (Ra) measurements.

	Surface chemical composition (atomic %)						Contribution in C 1s region (atomic %)		
Sample	**C 1s**	**N 1s**	**O 1s**	**Si 2p**	**Fe 2p**	**Cr 2p**	**Total polar groups (C-O, C=O and O-C=O)**	**WCA (°)**	**Ra (nm)**
SS AISI 316	53.99	1.33	33.56	ND	9.3	1.83	29.81	89.45	106
AP10	48.55	5.10	35.21	11.13	ND	ND	46.41	67.74	123
AP10+TE6	21	1.05	57.94	20.01	ND	ND	41.16	40.9	120
AP10+AA6	66.7	2.52	30.63	0.15	ND	ND	54.64	18.74	90.5
AP10+SA6	31.81	3.01	49.46	15.61	ND	0.11	43.97	37.15	105